

Effect of Phenolation, Lignin-Type and Degree of Substitution on the Properties of Lignin-Modified Phenol-Formaldehyde Impregnation Resins: Molecular Weight Distribution, Wetting Behavior, Rheological Properties and Thermal Curing Profiles

Marion Thébault¹, Larysa Kutuzova², Sandra Jury¹, Iris Eicher¹, Edith-Martha Zikulnig-Rusch¹ and Andreas Kandelbauer^{2,*}

¹Kompetenzzentrum Holz (Wood K Plus), Linz, A-4040, Austria

²Reutlingen University, Lehr- und Forschungszentrum Process Analysis & Technology, School of Applied Chemistry, Reutlingen, D-72762, Germany

*Corresponding Author: Andreas Kandelbauer. Email: andreas.kandelbauer@reutlingen-university.de

Received: 03 February 2020; Accepted: 25 March 2020

Abstract: Here, the effects of substituting portions of fossil-based phenol in phenol formaldehyde resin by renewable lignin from two different sources are investigated using a factorial screening experimental design. Among the resins consumed by the wood-based industry, phenolics are one of the most important types used for impregnation, coating or gluing purposes. They are prepared by condensing phenol with formaldehyde (PF). One major use of PF is as matrix polymer for decorative laminates in exterior cladding and wet-room applications. Important requirements for such PFs are favorable flow properties (low viscosity), rapid curing behavior (high reactivity) and sufficient self-adhesion capacity (high residual curing potential). Partially substituting phenol in PF with bio-based phenolic co-reagents like lignin modifies the physicochemical properties of the resulting resin. In this study, phenol-formaldehyde formulations were synthesized where either 30% or 50% (in weight) of the phenol monomer were substituted by either sodium lignosulfonate or Kraft lignin. The effect of modifying the lignin material by phenolation before incorporation into the resin synthesis was also investigated. The resins so obtained were characterized by Fourier Transform Infra-Red (FTIR) spectroscopy, Size Exclusion Chromatography (SEC), Differential Scanning Calorimetry (DSC), rheology, and measurements of contact angle and surface tension using the Wilhelmy plate method and drop shape analysis.

Keywords: Lignin; lignin-phenol-formaldehyde resin (PF); surface energy; viscosity; thermal characterization; design of experiments

1 Introduction

Phenolic (PF) resins used in the laminates industry are mainly water borne, liquid resols of low molecular weight with good penetration properties [1]. Resols are prepared under alkaline conditions with sodium hydroxide as a catalyst [2]. Since phenol is derived from fossil resources, alternative approaches



This work is licensed under a Creative Commons Attribution 4.0 International License, which permits unrestricted use, distribution, and reproduction in any medium, provided the original work is properly cited.

where renewable materials are exploited to substitute at least portions of the phenol monomer are desirable from an environmental point of view. Numerous studies aiming at replacing toxic and petroleum-based phenol by natural components were recently summarized [3]. Among these bio-based materials, lignins as the second-most abundant natural polymers, have an exceptionally high potential to replace petroleum-based phenol in PF resins [3–5]. Since lignin is a side product from various biorefinery and industrial processes such as the pulp and paper industry it is, in principle, available in large quantities and presents an economical substitute for phenol.

Lignins are high-molecular weight compounds consisting mainly of three basic monomers, sinapyl (S), guaiacyl (G) and para-hydroxy phenyl (H) alcohol (Fig. 1) that are cross-linked via different interconnections [3,6]. The relative proportions of the constituents and their configuration depend very much on the vegetable species the lignins are extracted from [7,8]. The chemical linkages in lignin are mainly ether bonds [9,10]. The main drawbacks of using lignin for phenolic resins are their lower reactivity due to their complex chemical structure and their smaller number of reactive sites compared to unsubstituted phenol as the starting material [11].

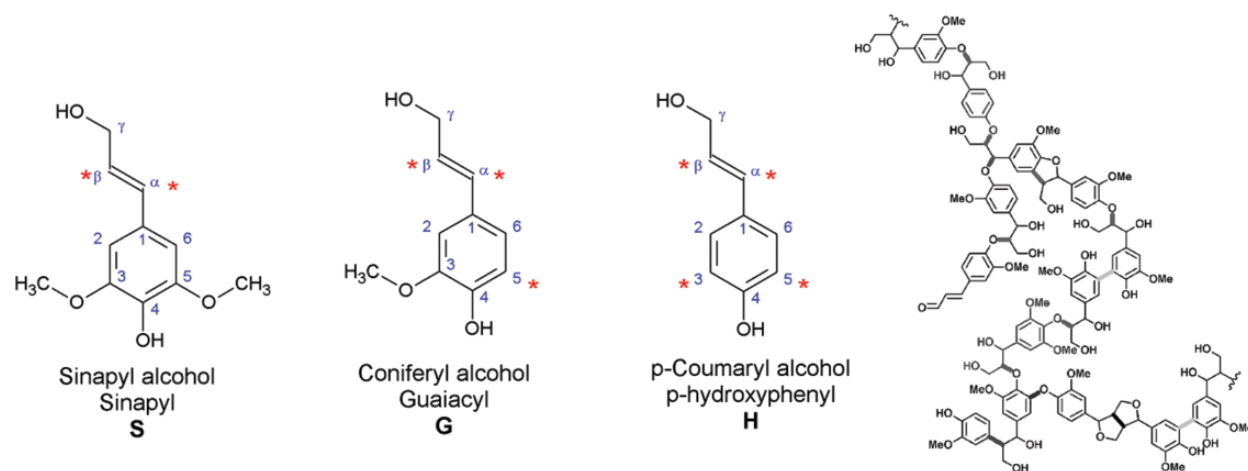


Figure 1: Chemical structures of the three main monomers in lignins (sinapyl S, guaiacyl alcohol G, and *p*-hydroxyphenyl, H monomers; the asterisks indicate nucleophilic reactive sites) and a typical structural representation of a softwood lignin

Methods to improve the reactivity of lignin include phenolation, alkylation and hydroxymethylation pretreatments [12] before incorporating lignin into a resin formulation. The phenolation treatment of lignins is carried out under acidic conditions and is supposed to lead to a partial depolymerization (“phenolysis”) of the high-molecular weight compounds via ether bond cleavage [11]. Thereby, a higher percentage of aromatic rings with a larger number of sites reactive towards formaldehyde becomes available [11,13].

Various studies on the preparation of phenolic resins with phenol-substitution by different sorts of lignin at different levels of replacements have been published where the resulting resins were assessed mainly for their gluing performance [14–17]. Only very few studies, however, deal with lignin-phenol hybrid resins that are especially suitable for paper impregnation as required for laminates manufacture [3,18–21]. With impregnation resins, homogenous impregnation of the porous network such as Kraft paper or glass fiber mats is very important. Inhomogenous impregnation could eventually lead to a number of defects in the final laminated board after hot pressing such as blisters, warping, delamination, etc. [22,23]. Therefore, with impregnation resins, besides rapid curing behavior (high reactivity) and sufficient self-adhesion

capacity (high residual curing potential), the flow behavior (viscosity) and the wetting properties (polarity) become especially important. The substitution of phenol by lignin can be expected to cause significant changes in these properties [24,25].

In the present study, several phenolic resins were prepared based on the basic synthetic protocol for a typical phenolic impregnation resin. They were modified with either one of two lignins of different provenience. The following three factors were studied at two levels: (1) lignin type (sodium lignosulfonate or Kraft lignin), (2) lignin pre-treatment prior to PF synthesis (with or without phenolation modification), and (3) phenol substitution level (either 30% or 50%). A 2-level-3-factor full factorial experimental design was applied to screen for the effects of these factors. The resulting lignin-phenol hybrid impregnation resins were characterized in terms of viscosity, surface energy and wetting behavior, molecular structure (FTIR spectroscopy), molecular weight distribution (GPC), and chemical reactivity (DSC).

2 Materials and Methods

2.1 Chemicals

Phenol (99% purity), formaldehyde (aqueous solution with a formaldehyde content of 37%) and sulfuric acid (96% aqueous solution) were supplied from Roth Chemicals (Karlsruhe, Germany). Sodium hydroxide was purchased from Sigma Aldrich (Saint-Louis, Missouri, United States). Sodium lignosulfonate DP 400 (L) was purchased from Westvaco Corp. (Charleston, South Carolina, United States), alkali lignin (Kraft, K) from Sigma Aldrich (Steinheim, Germany) and Indulin AT (Kraft, I) from Westvaco.

2.2 Resin Preparation

Resins were prepared according to a full two-level three-factorial experimental screening design using the factors (a) Lignin type (categorical factor, either Kraft lignin or lignosulfonate), (b) degree of substitution (numerical factor, either 30% or 50% substitution of phenol reaction mass), and (c) phenolation treatment (categorical factor, with or without phenolation). As a reference, a standard phenolic impregnation resin (P) was synthesized using a P:F molar ratio of 1:1.8. The degree of lignin substitution was calculated based on the mass of phenol required for this P:F ratio. The experimental settings for all prepared resins are given in [Tab. 1](#).

Table 1: Experimental settings used to prepare the various lignin-phenolic hybrid model resins synthesized with different types of lignin materials, treatments, and substitution levels

Resin	Substitution level (w/w Phenol)	Lignin material	Treatment before synthesis
PF	0%	–	–
L30PF	30%	Lignosulfonate	–
LP30PF	30%	Lignosulfonate	Phenolation
L50PF	50%	Lignosulfonate	–
LP50PF	50%	Lignosulfonate	Phenolation
K30PF	30%	Kraft lignin	–
KP30PF	30%	Kraft lignin	Phenolation
K50PF	50%	Kraft lignin	–
KP50PF	50%	Kraft lignin	Phenolation
I30PF	30%	Kraft lignin	–
IP30PF	30%	Kraft lignin	Phenolation
I50PF	50%	Kraft lignin	–
IP50PF	50%	Kraft lignin	Phenolation

The resins were prepared in a three-necked round bottom flask fitted with a temperature sensor, stirrer and reflux condenser. For all resins, the pH was adjusted to 8 by dropwise adding aqueous sodium hydroxide solution (45%). The flask was placed in an oil bath, heated under stirring to 90°C and kept under reflux for 120 min.

All lignin-phenol hybrid model resins were synthesized under the same reaction conditions (same pH, time and temperature) as the reference phenolic resin, except for that the phenol was partially (either 30% or 50% in weight) substituted by one of the two types of lignin (either Kraft lignin or lignosulfonate). The lignins were dissolved together with phenol and formaldehyde before heating. With half of the resins, a phenolation modification step was carried out prior to the actual resin synthesis for each lignin type and substitution level.

The phenolation treatment consisted of dissolving the lignin powder (37.5% w/w) with phenol (32% w/w) and water (30.5% w/w) by heating at 75°C for 1 h. Then, aqueous sulfuric acid solution (72% in H₂SO₄) was added (with a ratio H₂SO₄:phenol of 1:20 w/w) and the mixture was heated under reflux at 100°C for 3 hours. Afterwards, the mixture was cooled to room temperature and stored at 4°C until further use. For resin synthesis, the required amount of phenol to arrive at the desired substitution level was added and the mixture was stirred for one hour at 75°C. Then, the formaldehyde solution was added, and the pH was adjusted to 8 by adding sodium hydroxide solution. To remove liberated water, vacuum distillation was carried out after the synthesis.

2.3 Resin Characterization

2.3.1 Fourier Transform Infrared (FTIR) Spectroscopy

Fourier Transform Infrared Spectroscopy was performed with a Bruker TENSOR 27 apparatus (Bruker Optics GmbH, Ettlingen, Germany) fitted with a DuraScope SensIR detector. The spectra were recorded as an average of 32 scans with a double-sided forward-backward acquisition mode, in the spectral range between 4000 and 600 cm⁻¹ with a resolution of 2 cm⁻¹. All spectra were recorded from liquid resins.

2.3.2 Size Exclusion Chromatography (SEC)

All resin samples were dissolved in 5% w/w in dimethyl formamide (DMF). The measurements were carried out with a SEC column Jordi DVB-Glucose 10 000 Å, 5 µm, 300 × 7.8 mm, fitted with a pre-column Jordi GBR Mixed Bed 30 × 7.8 mm, on an HPLC Agilent 1100+ device. DMF was used as the eluent at a flow rate of 1.0 mL/min. Polystyrene standards having the following molar masses were used for calibration: 162, 685, 1470, 4700, 9130, 19600, 34800 and 100000 Da. The samples, each 25 µL at 20°C, were injected in the column, which was heated at 40°C. UV detection was done at 280 nm and a temperature of 35°C.

2.3.3 Surface Tension

Surface tension was measured with a DCAT11EC device from DataPhysics Instruments GmbH (Filderstadt, Germany) after dilution with methanol to a solid content of 45%. The measurement temperature was always 25 ± 1°C. The samples were thoroughly mixed before each measurement. At least four measurements per sample were carried out and the average values were calculated. The Wilhelmy Balance method [26] was used to calculate the surface tension with a plate PT11 made of platinum-iridium according to DIN 53914 standard.

2.3.4 Contact Angle Measurements

Contact angle measurements were carried out with the sessile drop method using an OCA 35 device from DataPhysics Instruments GmbH (Filderstadt, Germany). All measurements were carried out by depositing resin drops of defined volume on a flat glass microscopy slide (Carl Roth GmbH Co KG, Karlsruhe, Germany). The glass slides were cleaned with isopropanol prior to the measurements. Sessile drops of resins were produced using a syringe with a rate of 1 µl/s, approximately one millimeter above

the glass surface on which they were deposited. For determination of the contact angles, video documents were produced at 10 frames/second. The baseline of the glass surface was set manually. Contact angles were measured after the drops had stabilized from the droplet base-line. Contact angles were calculated as an average of the right and left angles. Measurements on each sample were repeated five times.

Using standard liquids (water, formamide and dichloromethane) with known surface properties at 20°C [27,28], the surface energy of the glass surface (γ_S) and its polar (γ_S^P) and dispersive (γ_S^D) components were determined with a series of liquid probes based on the Owens-Wendt-Rable-Kaeble (OWRK) model [28,29]:

$$\gamma_S = \gamma_S^P + \gamma_S^D \quad (1)$$

$$\gamma_L = \gamma_L^P + \gamma_L^D \quad (2)$$

$$\frac{1 + \cos \theta}{2} \frac{\gamma_L}{\sqrt{\gamma_L^D}} = \sqrt{\gamma_S^P} \sqrt{\frac{\gamma_L^P}{\gamma_L^D}} + \sqrt{\gamma_S^D} \quad (3)$$

where γ_L , γ_L^P , and γ_L^D represent the surface tension of the liquid and its corresponding polar and dispersive components, respectively, and θ is the contact angle. By plotting $(1 + \cos \theta)/2 * \gamma_L/(\gamma_L^D)^{1/2}$ versus $(\gamma_L^P/\gamma_L^D)^{1/2}$, the total surface energy of the glass was calculated to be 66.33 mN/m with a polar component of 48.72 mN/m and a dispersive component of 17.61 mN/m. The values of γ_L^P and γ_L^D for each lignin-phenol hybrid resin were obtained by extrapolation.

2.3.5 Viscosity

The solid content of the resins was adjusted to 45% by dilution with methanol. Dynamic viscosities of the samples were measured with a Physica MCR101 rheometer from Anton Paar, fitted with a conic spindle CP-50-1/01 of 50 mm diameter. The measurements were carried out by rotating the spindle from 1 to 100 s⁻¹ using some milliliters of resin sample in a metallic cup at a controlled temperature of 25°C. The Herschel-Bulkley I correlation method was used to determine the changes in viscosity with the shear rate; it was applied in the form $y = a + b \cdot x^P$.

2.3.6 Differential Scanning Calorimetry (DSC)

All thermograms were recorded using a differential scanning calorimeter 822e DSC (Mettler Toledo, Greifensee, Switzerland). 4 mg samples of the liquid PF and lignin-modified PF resins were subjected to a temperature gradient ranging from 25 to 250°C with a heating rate of 10 °C/min. To suppress evaporation of volatiles during condensation, the samples were sealed in high-pressure gold-coated stainless-steel crucibles of 30 µl total volume. The enthalpy changes were recorded and analyzed for the peak maximum temperature T_{peak} , the onset and endset temperatures T_o and T_e , and the normalized enthalpy integral ΔH , using the STAR 8.10 software package (Mettler Toledo, Greifensee, Switzerland). All measurements were repeated twice.

3 Results and Discussion

3.1 Structural Characterization by FTIR Spectroscopy

All prepared phenol-lignin hybrid resins were of light brown color (from honey-like to ochre-colored appearance), had a solid content after synthesis between 47 and 69% (see Tab. 2) and displayed a wide range of viscosities from ca. 14 to 300 mPa.s. (see Tab. 5). The nomenclature used in this manuscript for the prepared lignin-substituted PF resins was chosen as to reflect the lignin content and the type of treatment the lignin had experienced before preparing the actual PF pre-polymer. The first letter indicates the type of lignin and the second letter (if present) denotes whether the lignin was phenolated (or not, if no second letter is present). The number denotes the degree of substitution. Since all material data were

Table 2: Solid content, absolute and relative infrared peak area integrals and the estimated lignin content as calculated from the infrared spectra from the spectral range characteristic for aromatic skeletal group vibrations

Resin	Solid content after synthesis [%]	Peak area integrals from 1538–1164 cm ⁻¹		Calculated relative lignin fraction [%]
		Absolute	Normalized* [%]	
PF	52.1	53.3	100.0	0.0
L30PF	65.9	35.2	65.9	34.1
LP30PF	49.3	36.7	68.8	31.2
L50PF	66.9	29.4	55.2	44.8
LP50PF	47.3	27.6	51.7	48.3
K30PF	67.9	36.6	68.6	31.4
KP30PF	51.3	37.8	70.8	29.2
K50PF	68.9	26.2	49.1	50.9
KP50PF	49.0	26.2	49.1	50.9

Note: * Peak areas were normalized using the respective peak area integrals of unmodified PF resin as a reference

obtained from the phenol-lignin condensation products yielding liquid phenol-lignin resin pre-polymers, all assignments finish with “PF”. For instance, the assignment KP30PF reflects that the Kraft lignin was used, that the Kraft lignin was Phenolated before reacting it to the hybrid resin, and that a substitution degree of 30% was employed.

The FTIR spectra of all prepared resins are summarized in Fig. 2. In principle, they show all the same spectral features typical for phenolic resins but with different relative intensities. The absorbance bands that are characteristic for phenolic resins are the aromatic bands occurring at 3024 cm⁻¹ (aromatic ring vibration

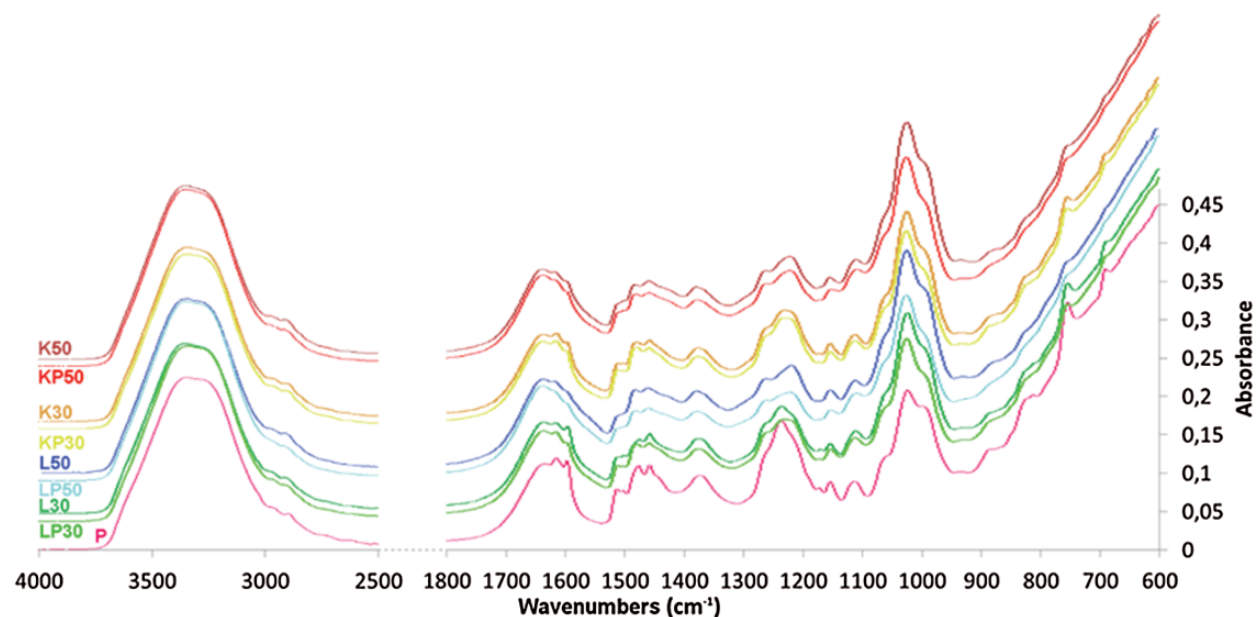


Figure 2: FTIR spectra of phenol-formaldehyde resins containing varying amounts of Kraft lignin or lignosulfonate

$\nu(\text{C-H})$), 1510 cm^{-1} ($\nu(\text{C=C})$), 1151 and 1112 cm^{-1} ($\text{dip}(\text{C-H})$); the phenolic bands at 1376 cm^{-1} ($\nu(\text{C=C})$), 1224 cm^{-1} ($\nu(\text{C-O})$), the aromatic C-H and/or C-O-C stretching at 1024 cm^{-1} and the methylene bridges at 1478 cm^{-1} ($\text{d}(\text{CH}_2)$) [30,31]. The bands at 1615 and 1600 cm^{-1} are ascribed to the aromatic carbon double bond stretching vibration. The shoulder observed at $1700\text{--}1635\text{ cm}^{-1}$ corresponds to carbonyl functionalities. As this vibration becomes more pronounced when the degree of phenol substitution increases, it may be related to the introduction of the lignin compounds. The absorbance signals at wavenumbers 690 , 756 , and 823 cm^{-1} correspond to the number of adjacent hydrogens on the phenolic aromatic ring: five, four and two H-atoms respectively.

A more detailed view of the FTIR spectra in the fingerprint region between $1700\text{--}920\text{ cm}^{-1}$ offers the possibility to estimate the degree of lignin substitution from the measured absorbance patterns. As an illustration, Fig. 3 shows the FTIR spectra for the Kraft lignin substituted-PF resins in the fingerprint region ($1700\text{--}920\text{ cm}^{-1}$) without normalization (a) and the total area-normalized FTIR spectra in the same spectral region (b). A semi-quantitative calculation of the lignin content in the prepared hybrid phenolic resins from infrared spectroscopic data was carried out via two approaches: (i) using the effect of “spectral dilution” of the absorbance intensities for the peaks typical of phenolic moieties carrying a substituent (data presented in Tab. 2) and (ii) evaluating the intensities of specific molecular segments of substituent (lignin-bands), these data are presented in Tab. 3.

The PF-based resin adhesives show the same IR-absorption profiles in the range of aromatic ring stretching ($\text{C}_{\text{aromatic}}=\text{C}_{\text{aromatic}}$, $\text{C}_{\text{aromatic}}\text{-H}$), phenolic and aliphatic hydroxyl groups ($\text{C}_{\text{aromatic}}\text{-OH}$, $\text{C}_{\text{aromatic}}\text{O-H}$, $\text{C}_{\text{aromatic}}\text{CH}_2\text{-OH}$ primary, $>\text{CH-OH}$ secondary) vibrations as well as vibrations that are characteristic for methylene ($-\text{CH}_2-$) bridges (Figs. 3a and 3b). The single peak area integrals or the sum of some peak area integrals of relevant absorbance signals in the region of the aromatic skeletal vibrations was used to quantitatively estimate the “dilution effect” on the peak intensities brought about by partial phenol substitution with lignin (Fig. 3c, Tab. 2). The data given in Tab. 2 show that the amount of lignin calculated from the area integral in the range of frequencies from $1538\text{--}1164\text{ cm}^{-1}$ directly correlates with the added amount of Kraft lignin.

For instance, the amount of 50.9% lignin calculated for the K50PF and KP50PF resins corresponds very well to the actual substitution level of 50%. Deviations from the expected values calculated for the lignosulfonate-substituted phenol-lignin hybrid resins can be explained by the presence of sulfonic acid groups, which contribute additional absorbance bands in the same spectral range ($1260\text{--}1150\text{ cm}^{-1}$) not present in the neat PF and Kraft lignin substituted resins [32].

It should be noted that Kraft lignin undergoes a more aggressive treatment during processing from the wood pulp raw material source than does lignosulfonate. Therefore, the degree of degradation (depolymerization) should be higher with the Kraft lignin. The additional phenolation of lignin should further reduce structural differences between pure PF and lignin-containing resins due to enhanced covalent bond formation with formaldehyde and a smaller amount of residual methoxyl groups. Figs. 3a and 3b show a significant decrease in intensity in the spectral region where lignin fragments typically absorb IR radiation: G-ring vibrations as well as vibrations of methoxyl groups at 1026 cm^{-1} [33].

The spectroscopically determined lignin fractions as calculated from several distinct spectral regions are compared in Tab. 3. Here, skeletal vibrations of phenolic compounds in the spectral range between 1538 and 1325 cm^{-1} and the vibrations of methoxyl groups in the spectral range from 1325 to 950 cm^{-1} were evaluated separately. It should be noted that the use of the aryl region in the broader boundaries allows very good correction of the baseline for the poorly resolved peaks. This improves the correspondence between the values calculated from the spectral profiles and the amount of phenolic compounds actually introduced. In contrast, the absorbance signal obtained from the lignin-specific methoxyl groups is only suitable to estimate the degree of substitution for the non-phenolized lignins. On the other hand, the partial

Table 3: Lignin fraction in the synthesized PF-lignin hybrid resins as calculated from absorbance integrals from FTIR spectra using different characteristic spectral regions

Resin	Lignin fraction, [%] calculated from peak area integrals			
	1090–945 cm ⁻¹ methoxyl groups	1135–950 cm ⁻¹ methoxyl groups	1533–1320 cm ⁻¹ aromatic skeletal region	1538–1164 cm ⁻¹ aromatic skeletal region
PF	0	0	0	0
L30PF	25.5	30.5	31.5	34.1
LP30PF	10.2	13.0	30.6	31.2
L50PF	45.2	27.5	41.7	44.8
LP50PF	9.5	18.4	46.6	48.3
K30PF	34.0	28.2	24.0	31.4
KP30PF	18.4	19.7	21.8	29.2
K50PF	50.8	43.1	38.0	50.9
KP50PF	22.6	30.2	39.2	50.9

demethylation taking place during the phenolation treatment can be quantitatively monitored and controlled using the signals in this spectral region. It should be noted that liginosulfonates can show slightly increased signal intensity in this region due to additional spectral contributions of vibrations of sulfonic acid groups. This is especially relevant at high degrees of phenol substitution by liginosulfonate.

3.2 Influence of Lignin Substitution and Lignin Phenolation Modification on the Molecular Weight Distribution of Lignin-Phenol Hybrid Resins

All produced phenolic resins and lignin-phenolic hybrid resins were examined for their molecular weight distribution by size exclusion chromatography (SEC). Low-molecular softwood kraft lignin Indulin AT was selected as a reference lignin because it is the most widely studied lignin type in literature. In [34], the dependence of the number of phenolic groups per molecule on the number of molecular weight fractions was studied in detail. The results obtained from the log-normal-curve fit of the HPSEC analysis showed that low molecular weight fractions with mass weights of 500 and 800 g/mol contain the numbers of phenolic groups per molecule (Ph-OH) 1.3 and 1.5, respectively, which is little different from pure phenol (1.14). As the MW fraction increases to 2000 g/mol, Ph-OH increases to 2.3. Considering that for Indulin AT M_n is 1457 g/mol with a polydispersion index of 6, the largest contribution to the mass distribution will be made by fractions with masses 500 (f1), 794 (f2), 1260 (f3) and 2000 (f4). The contribution of other high molecular weight fractions from 3000 will not exceed 0.1 [34] Our chromatographic measurements are in good agreement with the literature data for the unmodified Indulin AT (Fig. 4, sample I).

As can be further seen from Fig. 4, phenolation significantly improved the quality in terms of monodispersity and increased fraction of low-molecular weight compounds for all tested types of lignins (samples IP, LP, KP): each type of lignin shows a large low molecular weight fraction well below 500 Da.

The effect of introducing 30% and 50% raw and phenolated Indulin AT as a phenolic substitute into a phenolic resin is shown in Fig. 5a (samples I30PF and IP30PF) and Fig. 5b (samples I50PF and IP50PF). The mass distributions for the unsubstituted PF and the I30PF and IP30PF systems are very similar (Fig. 5a), except for that the relative proportion of the highest molecular weight fraction is much smaller in the case of the hybrid resins. This highest molecular weight fraction is only formed to the highest proportion in

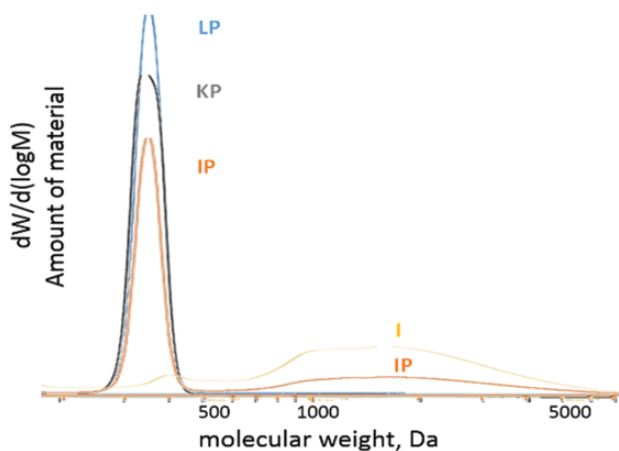


Figure 4: Molecular weight distribution of untreated Indulin AT (I), phenolated Indulin AT (IP), phenolated Kraft lignin (KP), and phenolated lignosulfonate (LP)

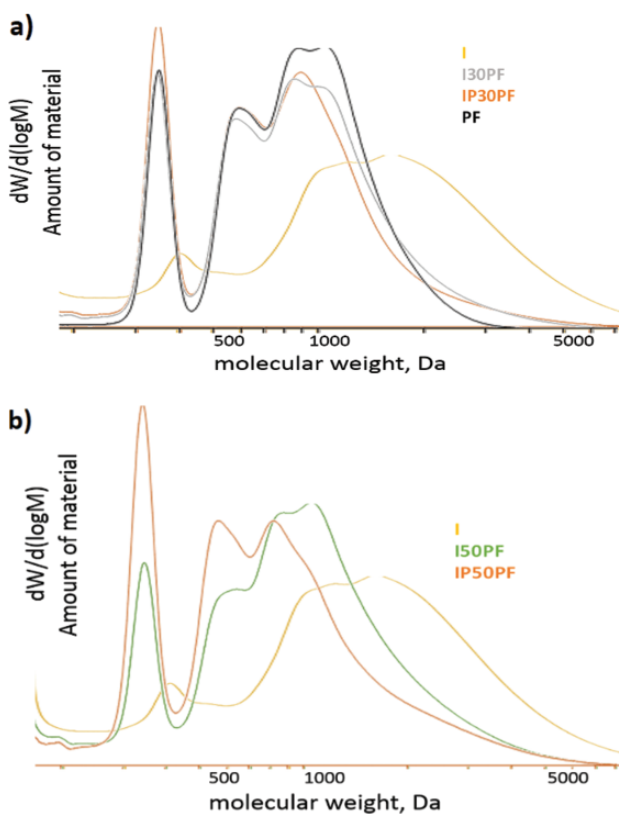


Figure 5: (a) Effect of phenolation on molecular weight distributions of low molecular weight Kraft lignin (Indulin AT, I), of pure phenolic resin (PF) as well as of hybrid resins with Indulin (I30PF) and with phenolated Indulin (IP30PF) with a phenol substitution of 30%; (b) Effect of phenolation on the molecular weight distributions of low molecular weight Kraft lignin (Indulin AT, I), and of hybrid resins with Indulin (I50PF) and with phenolated Indulin (IP50PF) with a phenol substitution of 50%

the homopolymerization reaction of P with F. The corresponding high molecular weight fraction of the hybrid resin containing the phenolated Indulin AT is even smaller as that of the one containing the unpretreated Indulin. Thus, if 30% of the phenol is substituted by either phenolated or unphenolated Indulin the molecular weight distributions of the resulting hybrid resins are only very much alike in the lower molecular weight region. The first three characteristic molecular weight fractions are formed in the ratio obtained also with the unsubstituted PF. The absence of the fourth higher molecular weight fraction indicates that the resulting resins are less suited for impregnation purposes as suggested by the favorable properties of the used reference PF resin. The absence of this fourth, high molecular weight fraction is particularly evident in the hybrid resin with phenol substitution of 50% (Fig. 5b, sample IP50PF).

It should be noted that at 50% phenol replacement by the unphenolated Indulin (sample I50PF, Fig. 5b) the residual amount of a high molecular weight lignin fraction also increased significantly as indicated by the broadening of the molecular weight distribution curve in the higher molecular weight region (2000–6000 Da). This indicates that, due to the limited solubility of the high molecular weight fraction, this fraction of the lignin had only been slightly chemically altered in the course of the phenolization reaction at pH 8.

Hence, one reason for the observed differences in molecular weight distributions of the various resins prepared in this study may be the differences in solubilities of the participating reaction partners. Norgren et al. [35] provide recommendations for avoiding coagulation in unmodified Kraft lignin in alkaline aqueous solutions at the different temperatures 21, 70 and 125°C. The pH values in such media (pH_{bulk}) should be at least 10 to maintain the highest degree of dissociation of the phenolic groups in the Indulin macromolecule. This pH_{bulk} is recommended based on the estimated pH_{surf} value, which represents the actual proton concentration at the fragment surface and is calculated using pK_a and the degree of dissociation of the phenolic groups. On the other hand, the low molecular weight fractions can be fully soluble at pH 7.5–9, whereas the high molecular weight fractions require a more alkaline medium and/or aqueous organic medium [36]. In the case of our synthesis conditions, the presence of organic monomers of phenol and formaldehyde as well as possible additional depolymerization in a hot alkaline medium [37] slightly improve the solubility of the lignin component of the hybrid matrix. This allows reducing the initial pH_{bulk} value to pH 8 in order to obtain oligomeric resins with good reactivity in condensation.

An additional stage of acidic phenolation of lignin before polymerization with phenol formaldehyde can significantly reduce the amount of high-molecular lignin fractions and improve the solubility and reactivity of lignin fragments (compare samples with and without phenolation). It should be noted that for this type of Indulin, the phenolation treatment according to the proposed scheme is not optimal because of the still high polydispersity of the resins: IP30PF and IP50PF contain significant amounts of several low-molecular weight fractions, and a significant residual amount of unmodified high-molecular lignin. The wide dispersion of the molecular weight (MW 300–6000), as well as the absence of fraction 4 as the main fraction, have led us to refrain from using this type of lignin in any further impregnation-related experiments.

It is interesting to note that the MW profile of the more polar lignosulfonate in the L30PF formulation has the same tendency as the I30PF (Fig. 6). Apparently, this is due to the fact that in moderately hot (75–90°C) slightly alkaline media in the absence of an additional oxidant, lignosulfonate will be only partially depolymerized [38] and its 30% substitution of synthetic phenol in the resin will also not be particularly active. A weak activation potential with a minimum number of active centers of raw lignosulfonates was also observed after phenol solution treatment in the absence of oxidizing agents and catalysts in [39].

Another equally valid reason for the decrease in the quality of the hybrid resins in terms of molecular mass distribution may be the change in reaction rate due to local variations of acidity at the surface of the lignin polyelectrolyte segments. It should be noted that the pH_{surf} may decrease by at least 0.5 pH units when the temperature increases from only 20°C to 70°C (under the assumption that the dissociation of the phenolic groups remains practically constant) [35]. Hence, in the case of our systems, it is fair to

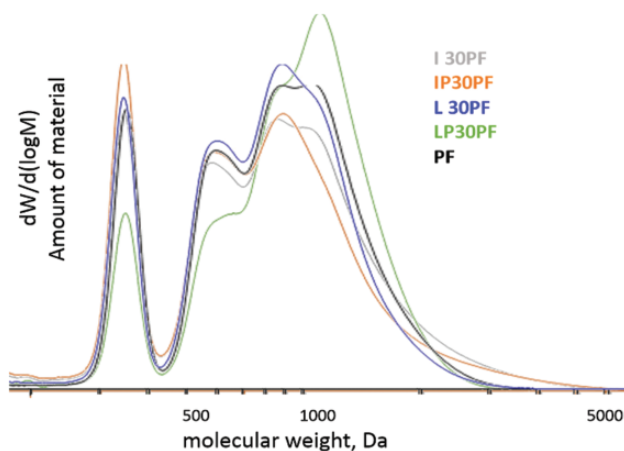


Figure 6: Effect of phenolation on the molecular weight distributions of different lignin type phenolic hybrid resins using (a) Kraft lignin Indulin without and with phenolation pretreatment (I30PF, IP30PF) and (b) lignosulfonate lignin without and with phenolation pretreatment (L30PF, LP30PF) with a phenol substitution of 30%. The sample of pure PF resin does not contain any lignin and is shown as a reference produced under the same preparation conditions

expect that already a small acidification of the medium due to local variations in surface pH of the lignin fragments under the applied conditions of hot alkaline synthesis of the hybrid resins will prevent obtaining the same molecular weight distribution as is obtained with the unmodified PF reaction mixture (see Fig. 6, samples I30PF, IP30PF, L30PF).

Therefore, a better explanation for the molecular weight increasing effect of phenolation is to consider small shifts in pH resulting from the addition of 30% by weight or more of phenolated lignin to the reaction mixture. The fact that the pH value has a very large influence on the molecular weight distribution is also shown by the molecular weight profiles of some related, purely phenolic resins which were prepared for comparison (Fig. 7). From the molar mass distributions of these unmodified phenolic resins, it can be

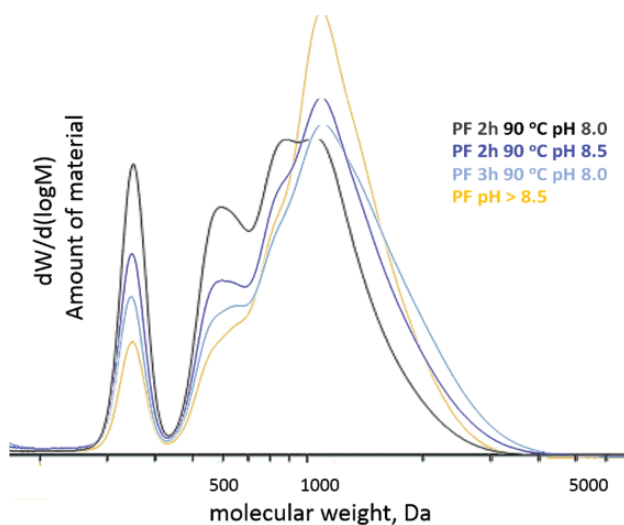


Figure 7: Molecular weight distributions of pure phenolic resins without lignin modification, but with different reaction time and initial pH values. PF8.0–2h: reaction time 2 hours at initial pH = 8.0; (b) PF8.5–2h: reaction time 2 hours at initial pH = 8.5; (c) PF8.0–3h: reaction time 3 hours at initial pH = 8.0; (a) PFpH > 8.5: commercially available PF resin. The reaction temperature was 90°C for all our PF

seen very clearly that even a small difference in the initial pH can lead to relatively large differences in the molar mass distribution after condensation (Fig. 7).

Already a shift of the initial pH value at the beginning of the synthesis by half a pH unit into the alkaline state from pH 8.0 to pH 8.5 resulted in the formation of a significantly higher proportion of oligomer fractions with a larger average molecular weight. Fig. 7 illustrates this for a series of four unmodified phenolic resins that were boiled for different lengths of time at two slightly different initial pH values. A longer boiling at lower pH had about the same effect as a shorter boiling at a correspondingly higher pH. Phenolic resin preparation is therefore very pH-sensitive with regard to the achieved molecular weight distributions. Accordingly, it is also to be expected that production-related fluctuations in pH during prepolymer synthesis will have a fairly significant effect on the molar mass distributions obtained and influence the processing and product properties.

Accordingly, even comparatively small changes in pH in the order of a few tenths of a pH unit should be significantly noticeable in molecular weight differences or higher degrees of condensation in the case of lignin-phenol hybrid resins. A possible cause for such pH shifts may be the release of reactive groups in the phenolation step. The generation of free alkaline groups in the lignin backbone should lead to an acceleration of the subsequent condensation reaction by a local increase of the pH value. We suspect that the hydrolysis of lignin fragments causes local pH shifts in the tenths of a pH range and that these already have a catalytic effect on the condensation reaction.

The fact that alkaline groups can be released in the course of phenolation was recently shown by Jiang et al. [40]. In their study, these authors also discuss several possible mechanisms that could determine the chemical processes taking place during the phenolation of lignin. Despite the fact, that collective pK_a -values of industrial lignins are 10.9 for a sulfate lignin, 10.5–11.0 for a Kraft lignin and 11.5 for the Kraft lignin Indulin-AT, the pK_a -values for different lignin-related phenolic groups have been found to vary in a range as wide as 6.2 to 11.3 [41]. The variations in the phenolic acidity of different oxidized substances can be extremely important in the pH catalyzed curing. Ragnar et al. 2000 give pK_a values for phenolic fragments that can be released during lignin degradation via phenolation and that are predominantly basic in nature [41]. In addition to a large number of basic groups, acidic groups can also occur, so that it is probably not always possible to speak of an alkalizing phenolation effect.

Fig. 8 shows the molecular weight distribution of Kraft lignin modified phenolic resins, where the Kraft lignin used was pretreated in different ways or added in different percentages. For comparison, the molecular weight distribution of two unmodified phenolic resins condensed at two slightly different initial pH values (pH = 8.0 and pH = 8.5) is also shown, as well as the molecular weight profile for the pure lignin starting material subjected to a phenolation step. Unfortunately, the corresponding non-phenolated lignin could not be measured under comparable analytical conditions due to its poor solubility in the elution medium. The molar mass profile of the phenolic lignin starting material shows very clearly the effect of pretreatment by phenolation on the molecular weight distribution: heating with phenol yields a low-molecular and above all very homogeneous (monodisperse) Kraft lignin. Phenolic resins with different lignin contents (30 and 50 weight % phenol substitution) were produced with such phenolic Kraft lignin (KP30PF and KP50PF in Fig. 8). In comparison to the phenolic Kraft lignin, it can be seen very clearly that the content of low-molecular weight compounds in the condensed lignin-phenol hybrid pre-polymer has significantly decreased. At the same time, the relative proportion of high-molecular condensation product has increased very strongly: compared to the analogous phenolic resin PF8.0 not modified with lignin, the fraction with the highest molecular weight is now much larger in the hybrid resins. Also, the molecular weight distribution became comparatively narrower. Moreover, the hybrid resins with phenolated Kraft lignin (KP30PF and KP50PF) differ from those with non-phenolated Kraft lignin (K30PF and K50PF) in their molecular weight. Again, with the hybrid resins K30PF and K50PF

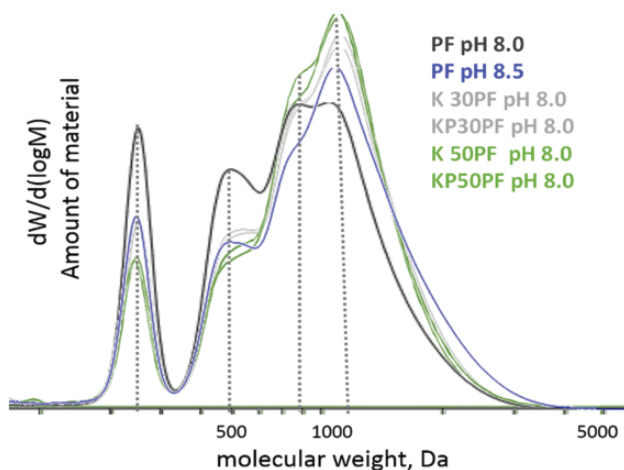


Figure 8: Molecular weight distributions of Kraft lignin-phenolic hybrid resins (K30PF, K50PF), of phenolated Kraft lignin-phenolic hybrid resins (KP30PF, KP50PF) and of various comparison phenolic resins without added lignin (PF). The preparation of the unsubstituted phenolic resin was carried out at 90°C for 2 hours with an initial pH of pH 8.0 (PF pH8.0) or pH 8.5 (PF pH8.5). The preparation of the Kraft lignin-phenol hybrid resin was also carried out at 90°C and 2 hours reaction time, but always with an initial pH_{bulk} of 8.0 and different lignin substitutions 30 and 50%

modified with non-pretreated lignin an average increase in the fraction of high molecular weight compounds can be observed compared to the corresponding pure phenolic resin PF8.0. However, the fractions with low and medium molecular weight are still comparatively larger than in the corresponding hybrid resins KP30PF and KP50PF produced with phenolated Kraft lignin. Thus, by the phenolation pretreatment of the starting Kraft lignin an even further increase of the fraction of high molecular weight components has been achieved. A similar behavior was observed in the case of the replacement of 50% phenol by lignosulfonate. Here, too, the substitution with a lignosulfonate pretreated with phenolation led to a completely analogous quantity-dependent increase in the proportion of higher molecular weight compounds. A larger quantity of phenolated lignosulfonate resulted in a larger proportion of higher molecular weight fragments.

Thus, by condensing Kraft lignin into our impregnating resins, the average molecular weight of the resulting lignin phenolic hybrid resin was always increased, regardless of the pre-treatment of the Kraft lignin. The average molecular weight increase of PF resins due to the addition of pre-condensed lignin-oligomers could still be explained simply by the fact that a certain amount of higher molecular weight starting materials was added to the PF right at the start of the synthesis. However, since the Kraft lignin after phenolation is actually of quite low molecular weight (Fig. 4), the overall increase in average molecular weight of the hybrid resins obtained with the phenolated lignin cannot solely be explained on such a basis. Fig. 4 shows that, for example, already a shift of the initial pH by half a pH unit in pure phenolic resin from pH 8.0 (PFpH8.0, Fig. 8) to pH 8.5 (PFpH8.5, Fig. 8) leads to a shift in the molecular weight distribution, which results in a mass profile very similar to those of the Kraft lignin-substituted ones (compare Fig. 7 PFpH8.5 with the lignin-containing hybrid resins).

Fig. 9 schematically summarizes the presumed effect of phenolation on the morphology of the liquid pre-polymers in PF-lignin hybrid resin preparation. Upon phenolation, the number of reactive sites in lignin increases due to depolymerization which is accompanied by liberation of basic groups that cause local alkaline pH shifts. The differences between the hybrid resins with Kraft lignin, lignosulfonate and indulin make it clear that phenolation of lignin may yield rather complex oligomer mixtures, which can

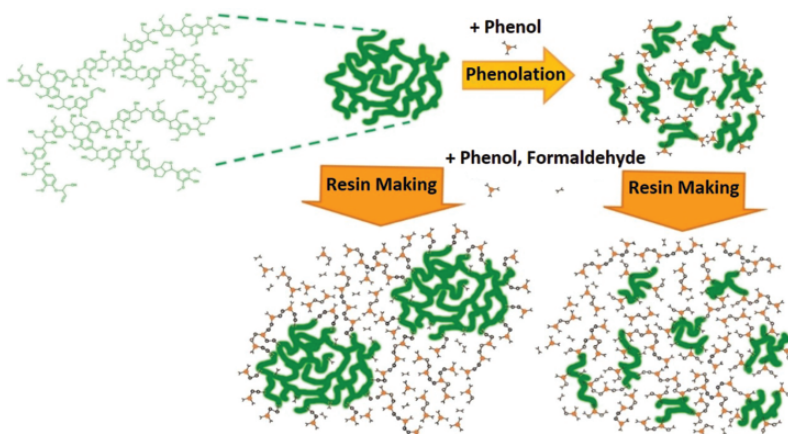


Figure 9: Schematic representation of the effect of phenolation on resin morphology of the liquid prepolymer

have quite different effects on the further course of phenolic resin condensation depending on the specific reaction conditions and the provenance of the starting lignin. With Kraft lignin and lignosulfonate, phenolation seems to lead to an activation of the lignin and thus to an increase of its reactivity towards further condensation. Therefore, further experiments for the production of impregnating resins were only conducted with lignosulfonate and Kraft lignin.

3.3 Effect of Lignin Substitution on the Wetting Properties

The wetting behavior of the prepared resins was measured using tensiometry and contact angle measurements. In the case of the purely phenolic reference resin, the resin drops spread to such a large extent on the glass surface that the contact angle could not be derived from the video images. This means, however, that the contact angle of the reference PF resin is very low. The values for surface tension, contact angle with glass as a reference surface and the polar and dispersive components of the surface energy are summarized in [Tab. 4](#).

Table 4: Surface tension (γ_L^{tot}), contact angle (CA), and polar (γ_L^P) and dispersive (γ_L^D) components of the surface energy for the phenolic resins

Resin	CA (°)	γ_L^{tot} * (mN/m)	γ_L^P (mN/m)	γ_L^D (mN/m)
PF	N.D.**	32.17	–	–
L30PF	26.5	30.83	0.79	30.04
LP30PF	28.4	32.25	0.96	31.29
L50PF	25.0	28.71	0.53	28.18
LP50PF	34.1	30.88	0.53	30.35
K30PF	25.3	29.69	0.66	29.03
KP30PF	22.6	33.41	1.45	31.96
K50PF	38.1	33.55	0.72	32.83
KP50PF	24.4	33.04	1.29	31.75

Note: * upon water removal and solid content adjustment to 45% with methanol. Experimental error of contact angle values was from 1.7 to 2.8 angle units.

All studied phenol-lignin hybrid resin liquids showed a very high dispersive surface energy component, γ_L^D , compared to their polar surface energy component, γ_L^P . Hence, the total surface energy of the resins, γ_L^{tot} , was mainly governed by the dispersive surface energy component and was directly proportional to γ_L^D (Fig. 10c).

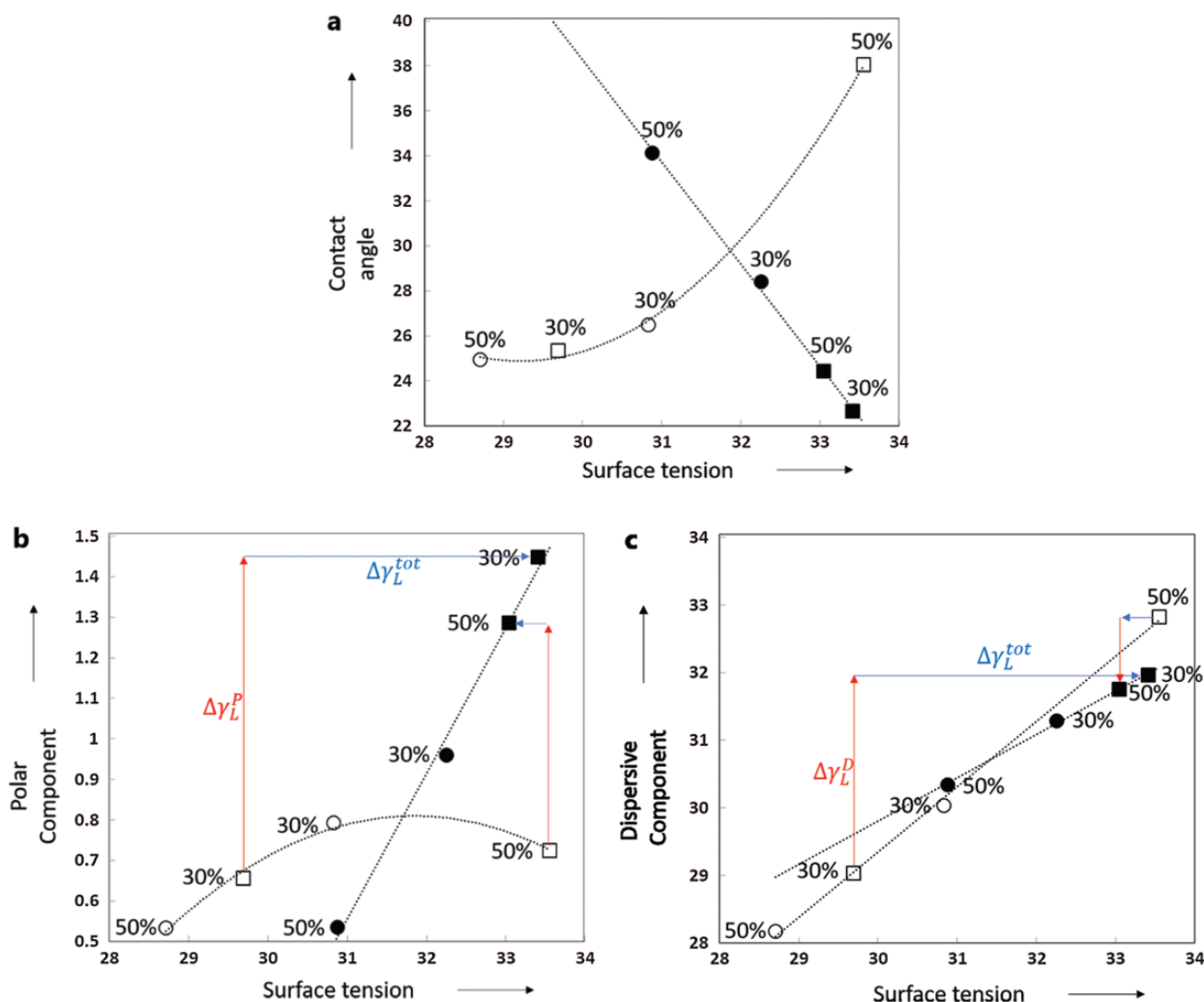


Figure 10: (a) Contact angle vs. surface tension values for the lignin-phenolic hybrid resins. (b) Polar component of surface tension. Circles (\circ , \bullet) represent lignosulfonate and squares (\square , \blacksquare) represent Kraft lignin containing lignin-phenolic hybrid resins. Open symbols represent resins without phenolation modification, black symbols represent resins that were phenolated

Compared to the unsubstituted resin, substitution of phenol by lignosulfonates yielded mostly resins with slightly lower surface tension whereas substitution with Kraft lignin gave mostly resins with slightly higher values. Similar results were found earlier by Matsushita et al. [25] who used inverse gas chromatography and contact angle measurements of solid films made of phenolic resins that were partially substituted by similar types of lignin materials. However, the measured differences in contact angles and surface tension in our present study did not reveal statistically significant effects of the studied factors in the ANOVA when the average values for the wetting properties were used in the analysis

except for the response γ_L^P . γ_L^P showed some weakly significant correlation with the two factors “phenolation” ($p = 0.0447$) and “lignin type” ($p = 0.0702$) and their second order interaction ($p = 0.0879$) at the significance level of 0.1. This result was mainly due to the comparatively larger polar components of the two Kraft-lignin containing resins that had experienced phenolation modification.

However, an instructive view on the structure of the data set is revealed by the scatter plot of the tensiometer values for surface tension, γ_L^{tot} versus the contact angle (Fig. 10a). For the phenolated resins, the contact angle decreased linearly with increasing γ_L^{tot} . A higher degree of substitution resulted in lower surface tension values and correspondingly increased contact angles. The phenolated resins containing Kraft lignin wetted the glass surface generally better than the phenolated resins with lignosulfonates. Moreover, phenolation improved the wetting behavior of the resins containing Kraft lignin whereas it caused a decrease in wetting with the lignosulfonate containing resins. Both effects were more pronounced with a higher degree of substitution.

The lignin-phenolic hybrid resin containing 50% of Kraft lignin showed the largest difference in contact angles between the phenolated resin and the one without modification. This phenolated resin wetted the glass surface much better than its counterpart without modification. Although the phenolated and the non-phenolated resins had practically the same surface energy (33.05 and 33.55 mN/m, respectively), their contact angles differed by as much as 14°. Since these two resins also showed practically the same molecular weight, phenolation in this case had caused a shift in the ratio between polar and dispersive surface energy components towards more favorable wetting conditions without significantly changing the overall Kraft lignin molar mass. While γ_L^P increased upon phenolation, γ_L^D decreased at the same. Both changes were in favor of improved wetting but left the absolute value of γ_L^{tot} practically unchanged. For illustration, in Fig. 10b, the relative changes in γ_L^{tot} and γ_L^P upon phenolation are indicated with red and blue arrows for the Kraft lignin containing PF hybrid resins. This is in good agreement with the increasingly important phenolytic effect of the phenolation modification treatment at the lower level of lignin substitution observed with the polydispersity index: obviously, phenolysis liberates relatively more polar species at the lower degree of substitution.

The relative increase in γ_L^P was even higher with the 30% Kraft lignin resin. However, the corresponding improvement in surface wetting was much less pronounced here. Phenolation had caused an increase in the dispersive component, γ_L^D , too, which is superimposed to the increase in γ_L^P and counteracted its effect on the total surface energy, γ_L^{tot} correspondingly. The relative changes in γ_L^P and γ_L^D become even more unfavorable for the wetting behavior of the lignosulfonate-based hybrid resin. With lignosulfonate, phenolation even leads to a slight increase in contact angle for both levels since the increase in γ_L^P is practically negligible and overcompensated by the increases γ_L^D . As with Kraft lignin, the relative changes in γ_L^P are more pronounced at the lower level of lignin substitution.

3.4 Effect of Lignin Substitution on Viscosity

The dilution of a polymer in a solvent can completely change the viscosity behavior of a resin, as observed in data of a previous work [42]. This relates to the chemical interactions between the polymer molecules between themselves and the solvent. The shear stress and viscosity plots with shear rate (Fig. 11) show the viscous behavior of each prepared resin system as liquids diluted with methanol (Tab. 5).

The observed behavior is rather complex. At the higher level of substitution (50%), the resins without lignin phenolation become more viscous. All resins with substitution by lignin present a slight to significant increase in viscosity compared to the non-substituted phenolic resin P. With some resins, the evolution of viscosity with the shear rate was not progressive. A pseudo-periodicity that disturbed the rotation of the spindle was notable for L50PF, LP50PF, K30PF and K50PF. This indicates the presence of particles in these liquids. For most of the resins, the behavior was dilatant or shear thickening (e.g., the viscosity increases with the shear rate): the lignin in the resins obviously tended to form aggregates, which

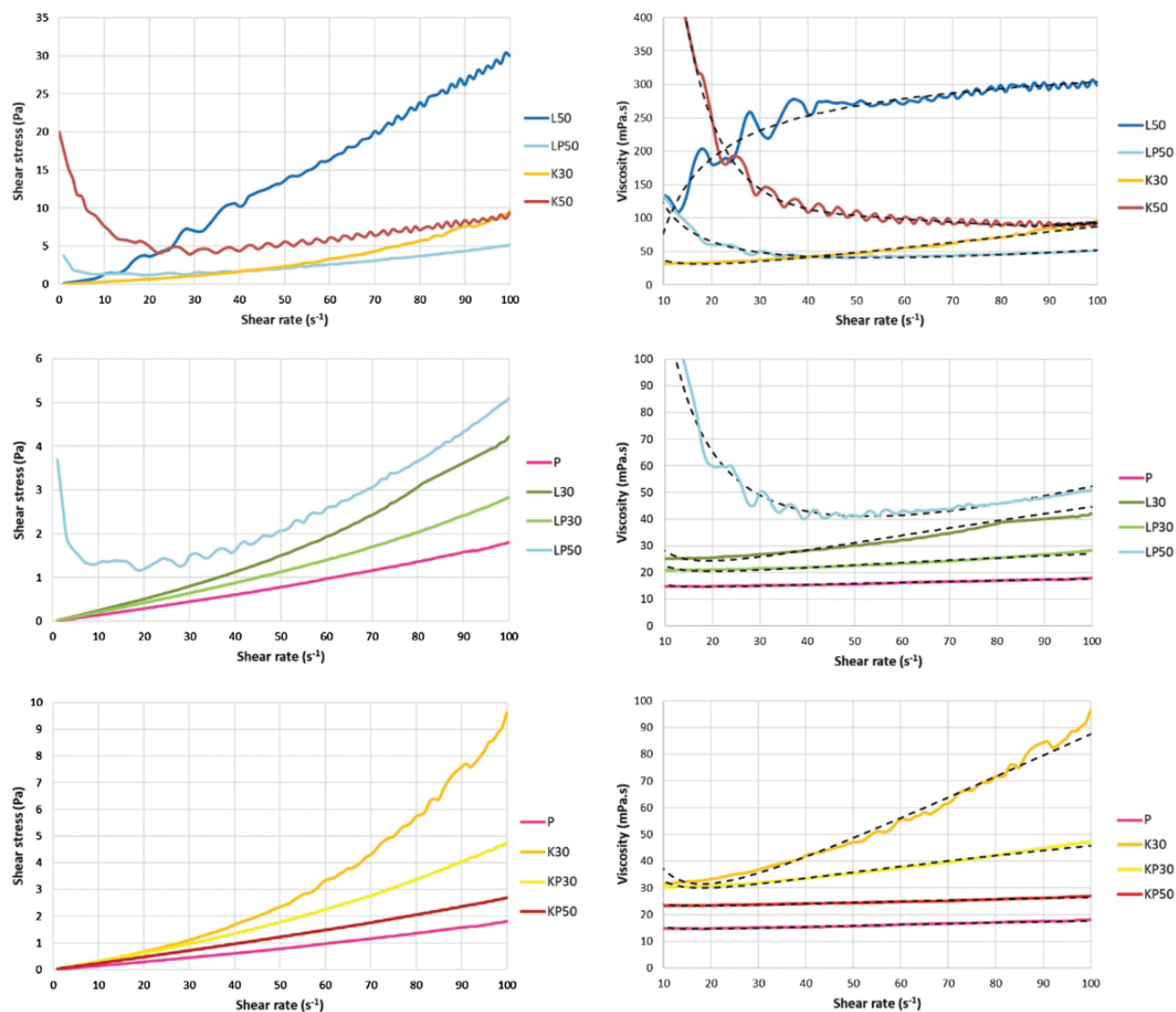


Figure 11: Plots of shear stress (on the left) viscosity values (on the right) with shear rate of each resin system diluted in methanol (45% w/w of solid content). The dashed lines corresponds to the models calculated according to the Herschel-Bulkley I method, except for K50PF (4th polynomial I method)

produced suspensions in the liquid. Exceptions were encountered with resins LP50PF and K50PF, where the viscosities had initially higher values, which decreased with the shear rate. Concerning K50PF, the evolution of the viscosity profile was typical of a Bingham plastic fluid [22], whereas the resin L50PF had a pseudoplastic (or shear-thinning) behavior, which is often seen in polymers in solution that are entangled at rest but start to disentangle when sheared at a sufficiently high rate because of weak interactions. In the case of LP50PF, the viscosity decreased until a minimum value around 50 s^{-1} , which suggests a Bingham liquid behavior and then increased slightly like a low-dilatant fluid. This dual effect could be due to a mixture of cohesive high-molecular weight compound (responsible for the Bingham profile) and resin particles that are in suspension in the methanol solvent (which is typical for dilatant fluids).

Statistical analysis of the viscosity measured at 100 s^{-1} reveals some interesting relationships and illustrates the complex effects of the studied factors on the rheological behavior of the lignin-phenol hybrid resins. The results of the ANOVA are summarized in Tab. 6. A highly significant two-factor

Table 5: Viscosity data of resins diluted in methanol (45% w/w), using the Herschel-Bulkley I correlation method

Resin	Viscosity 20 s ⁻¹ (mPa.s)	Viscosity 50 s ⁻¹ (mPa.s)	Viscosity 100 s ⁻¹ (mPa.s)	Viscous profile
PF	14.6	15.8	17.7	Newtonian-Dilatant
L30PF	24.4	31.1	44.6	Dilatant
LP30PF	20.6	22.9	27.1	Dilatant
L50PF	190	268	304	Shear-thinning
LP50PF	65.3	41.1	52.3	Bingham-Dilatant
K30PF	31.6	48.7	87.5	Dilatant
KP30PF	30.1	35.9	45.9	Dilatant
K50PF	246*	104*	94.4*	Bingham
KP50PF	23.3	24.5	26.5	Newtonian-Dilatant

Note: *Using the 4th Polynomial I correlation method

Table 6: ANOVA analysis of the effects influencing the response “viscosity at 100 s⁻¹” for the studied lignin-phenol hybrid resins

	<i>F</i> -value	<i>p</i> -value	R ²	R ² _{adjusted}	R ² _{predicted}
Model	215.47	0.0046	0.9981	0.9935	0.9704
Effects	Coefficient estimates (coded):				
A: Lignin type	1.82	0.3097			-0.0018
B: Phenolation	586.50	0.0017			+0.0319
C: Substitution	96.44	0.0102			-0.0129
AC	320.98	0.0031			-0.0236
BC	71.59	0.0137			+0.0112

Note: Statistical analysis was performed after reciprocal square root data transformation

interaction model ($p = 0.0046$) describes this response very well as indicated by all three regression coefficients R^2 , R^2_{adjusted} and $R^2_{\text{predicted}}$ which are all very close to 1 (Tab. 6). The model contains all three studied factors and two second-order interactions. Lignin type in itself does not seem to be statistically significant. However, lignin type must be included in the model since it is involved in a highly significant synergistic effect with the degree of substitution. This two-factor interaction is the second most important effect determining the viscosity of the system, as can be seen from the coefficient estimates for the various effects summarized in Tab. 6. The most important effect is whether the phenolation modification is performed or not. Being of the same order of magnitude, the third most important effects then are the degree of substitution of phenol by lignin and its synergistic action with the phenolation modification. Since there are two second-order interaction effects present, it is not surprising that the rheological behavior of lignin-phenol hybrid resins is rather complex and difficult to understand.

Fig. 12 depicts the interaction plot for the largest synergistic effect for the response obtained without phenolation modification (Fig. 12a) and with phenolation (Fig. 12b). While the viscosity of unphenolated Kraft-lignin-containing PF resin is not significantly influenced by the amount of phenol substitution by Kraft lignin, the amount of lignosulfonate present dramatically increases resin viscosity when no

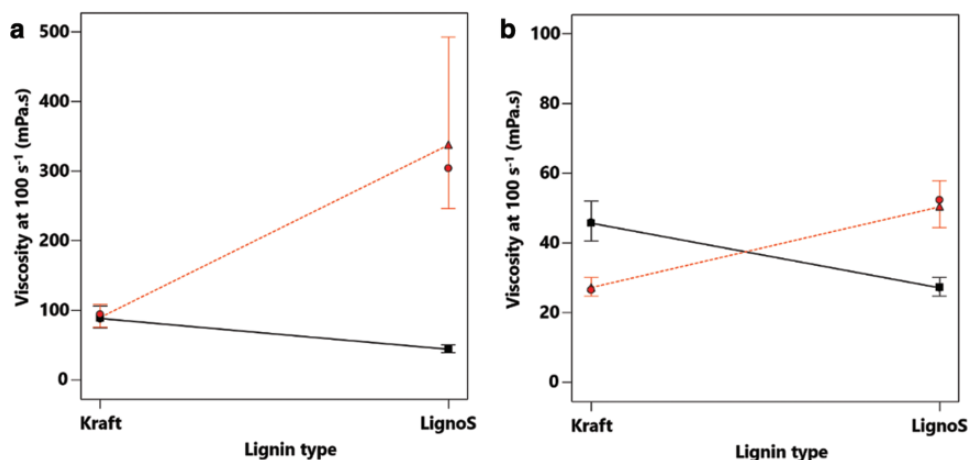


Figure 12: Two-factor interaction plot for viscosity at 100 s^{-1} for the synthesized lignin-phenol hybrid resins. (a) without phenolation, (b) with phenolation treatment. The black squares and the full line represent the low level of substitution (30% lignin). The red triangles and the dotted red line represent the high level of substitution (50% lignin) derived from the model. Correspondingly colored circles represent the actually measured values

phenolation modification is performed. However, phenolation decreases the viscosity of all resins dramatically (please note the different scales in Figs. 12a and 12b!). This is also in line with the presumed phenolytic depolymerization action of the phenolation treatment (Fig. 9). Phenolation, thus, levels off greatly the effects of both lignin type and lignin amount and should be carried out in order to adjust resin viscosity to reasonably low values if good resin flow properties are required. In terms of viscosity, phenol can be substituted to fairly high degrees without increasing resin viscosity to undesirably high levels as long as a phenolation treatment step is included in the resin formulation process.

3.5 Effect of Lignin Substitution on Thermal Properties

3.5.1 Effects on the Responses ΔH_1 and ΔH_2

The thermal properties of the lignin-phenol hybrid resins were analyzed with DSC. The exothermal curing profiles (i.e., DSC traces) of PF resins typically depend on the condensation conditions of the resins (P:F ratio, catalyst nature and content, heating temperature and duration) and are indicators for their reactivity and curing kinetics. Fig. 13 collects the DSC traces of all prepared PF and lignin-modified PF impregnation resins. The corresponding reaction enthalpies, onset, peak and endset temperatures are listed in Tab. 7.

With all resins, two exothermal enthalpy peaks were obtained: the first exothermal peak was rather broad for all resins and occurred in the temperature range from 125°C to 190°C . The second exothermal peak was comparatively sharper for all lignin-modified resins and rather broad for the phenolic reference resin. It occurred in the temperature region between 210°C and 230°C . For relatively slowly curing PF resins, an exothermal peak temperature in this range is typically found in the literature [43,44].

In their 1985 Design-of-Experiment study on the influence of reaction parameters on PF resin properties, Christiansen et al. [45] had also found two exothermic peak maxima in the DSC traces of their liquid resins. They had assigned the first peak maximum (very sharp, found between 98 and 129°C) to the addition reaction between phenol and formaldehyde (methylolation). The second exothermic peak maximum which was much broader in their case was found between 139 and 151°C and was assigned to the condensation reaction [45].

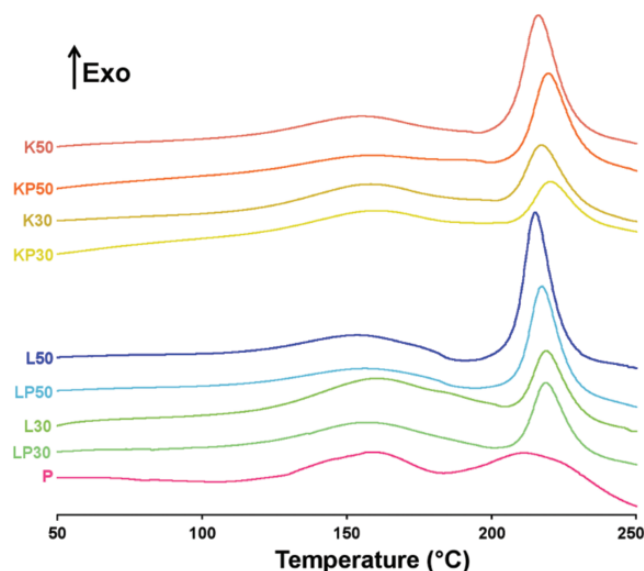


Figure 13: DSC curves of the different resins at a heating rate of 10 °C/min

Table 7: Normalized enthalpies, ΔH_1 and ΔH_2 , onset temperatures, $T_{o,1}$ and $T_{o,2}$, peak temperatures, $T_{peak,1}$ and $T_{peak,2}$, and endset temperatures, $T_{e,1}$ and $T_{e,2}$ obtained from the DSC thermograms of the phenol-lignin model resins. The term $\Delta H_{tot}(= \Delta H_1 + \Delta H_2)$ is also included

Resin	$T_{o,1}$ (°C)	$T_{peak,1}$ (°C)	T_{e1} (°C)	ΔH_1 (J/g)	T_{o2} (°C)	$T_{peak 2}$ (°C)	T_{e2} (°C)	ΔH_2 (J/g)	ΔH_{tot} (J/g)
PF	127.38	157.31	179.90	74.00	194.37	212.65	239.06	48.01	122.01
L30PF	136.33	159.59	196.54	93.35	210.20	219.04	230.92	65.39	158.74
LP30PF	119.16	156.63	193.21	73.89	209.63	218.49	230.15	69.27	143.16
L50PF	118.37	155.34	186.53	67.83	207.36	215.44	225.54	151.81	219.64
LP50PF	120.13	156.51	173.88	70.92	208.85	217.17	227.58	105.40	176.32
K30PF	123.87	157.73	184.70	57.28	207.60	217.84	231.67	80.06	137.34
KP30PF	135.05	158.88	184.75	46.58	210.99	220.76	234.17	48.42	95.00
K50PF	121.62	156.75	195.44	63.48	207.19	216.98	228.81	134.85	198.33
KP50	119.57	154.91	190.48	36.28	210.11	219.65	231.87	101.02	137.30

The authors used liquid resols and systematically changed the sodium hydroxide portions during synthesis in order to adjust differently methylolated and pre-condensed reaction species.

As an alternative interpretation, Park et al. [46] suggested to relate the two exothermic enthalpy maxima and their corresponding temperature ranges to the average molecular weight distribution of PF resins: while reactive species with a higher molecular weight presumably should cure at a lower temperature, smaller species should require higher temperatures for curing. Hence, if the resin contained different fractions of molecular weights, it would display two major exothermic peaks in the DSC thermograms [46].

In our case, all lignin-phenolic hybrid resins showed a much larger second exothermic curing enthalpy signal ΔH_2 than the reference phenolic resin (except for the one containing Kraft lignin at the 50% degree of substitution level with the phenolation treatment: with the latter it was in the same order of magnitude). At the

same time, nearly all lignin-phenolic hybrid resins had comparatively lower ΔH_1 -values (except for the non-phenolation treated 30% lignosulfonate containing one) reflecting the partial substitution of phenol raw material. This finding suggests that ΔH_2 in our case should rather be assigned to the curing of a higher molecular weight fraction.

This interpretation would also make sense since higher molecular weight compounds are less mobile and hence should require more energy to overcome activation energy barriers in a diffusion-controlled reaction regime. The relative proportion of the higher molecular weight fraction increased with increasing the level of phenol substitution as did ΔH_2 : the integrals ΔH_2 in the higher temperature region between 210 and 230°C were always larger for the resins with 50% of phenol substitution compared to those with only 30% of phenol substitution, whether they were phenolation modified ($\Delta H_{2,LP50PF} > \Delta H_{2,LP30PF}$, $\Delta H_{2,KP50PF} > \Delta H_{2,KP30PF}$) or not ($\Delta H_{2,L50PF} > \Delta H_{2,L30PF}$, $\Delta H_{2,K50PF} > \Delta H_{2,K30PF}$). ΔH_2 at 50% substitution was always larger than 100 J/g. At 30% substitution it was always ≤ 80 J/g. Phenolation treatment led to statistically significantly smaller values.

The analysis of variance for the responses ΔH_1 and ΔH_2 are summarized in [Tabs. 8 and 9](#). Only the significant terms are given. The corresponding model graphs including all measurement points are given in [Figs. 14a and 14b](#).

Table 8: ANOVA of effects on the response (ΔH_1) for the studied lignin-phenol hybrid resins

	Sum of Squares	F-value	p-value	R ²	R ² _{adjusted}	R ² _{predicted}
Model ^{*)}	1309.95	9.49	0.0217	0.6126	0.5480	0.3113
Effects				Coefficient estimates (coded):		
A: Lignin	0.0217	9.49	0.0217			-22.96
Residual	828.41					

Table 9: ANOVA of effects on the response (ΔH_2) for the studied lignin-phenol hybrid resins

	Sum of Squares	F-value	p-value	R ²	R ² _{adjusted}	R ² _{predicted}
Model ^{*)}	8067.05	2453	0.0026	0.9075	0.8704	0.7631
Effects				Coefficient estimates (coded):		
B: Phenolation	1458.00	8.86	0.0309			+13.50
C: Substitution	6609.05	40.17	0.0014			-28.74
Residual	822.65					

Lignin type was the only significant term affecting the first exothermic enthalpy signal, ΔH_1 , lignosulfonate yielding larger ΔH_1 . Besides phenolation treatment, the main effect for ΔH_2 was the degree of substitution by lignin. A larger degree of substitution led to an increased exothermic enthalpy signal. The phenolation modification had a counteracting effect since it resulted in a decrease in ΔH_2 for both lignin types. Lignin type had no significant effect with ΔH_2 . Absolute values for ΔH_2 were generally higher than those for ΔH_1 (please note the different scales for the enthalpy signal in [Figs. 14a and 14b](#)).

3.5.2 Effects on the Total Residual Curing Capacity ΔH_{tot}

The most relevant thermal property of the impregnation resin is presumably its residual curing potential which is measured by DSC as the total exothermic enthalpy change, ΔH_{tot} . ΔH_{tot} was calculated as the sum

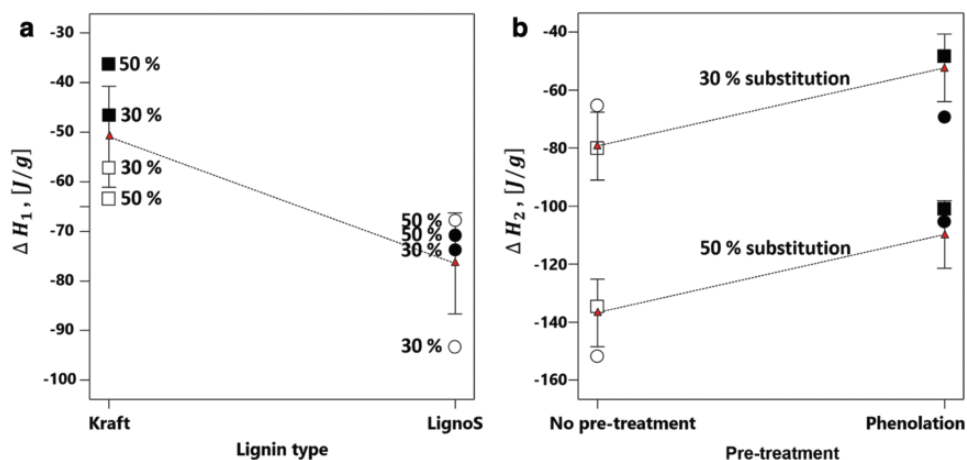


Figure 14: Interaction plot for (a) the effect of lignin type on the first exothermic peak integral, ΔH_1 , and (b) the effects of phenolation treatment and the degree of phenol substitution on the second exothermic peak integral, ΔH_2 . Circles (\circ , \bullet) represent lignosulfonate and squares (\square , \blacksquare) represent Kraft lignin containing lignin-phenolic hybrid resins. Open symbols represent resins without and black symbols resins with phenolation treatment. Triangles represent the average values

of the two exothermic peak integrals ΔH_1 and ΔH_2 observed in the DSC trace and is a measure of the resin's overall potential for self-gluing upon heating when the resin impregnated paper sheets are hot-pressed into a decorative laminate. Since no additional glue is applied during lamination, good self-gluing ability is desired and the resin should display sufficiently high values for ΔH_{tot} .

Practically all lignin-phenol hybrid model resins displayed a higher residual curing capacity ΔH_{tot} than the pure phenolic resin (except for the KP30PF resin). Since all resins were prepared at the same reaction time, this means that the reference PF resin was already at a more progressed condensation state after synthesis than the lignin-modified ones. This would be expected since phenolic resins are more reactive than lignin-modified ones due to the higher number of reactive sites available.

Among the lignin-modified resins, the non-phenolated ones with high degrees of phenol substitution showed the highest values whereas the phenolated ones with low degree of substitution showed the lowest ones. This correlates with the expected reactivity of the lignins during resin synthesis: high contents of lignin would result in lower conversation rates which in turn would lead to higher residual curing capacity. In contrast, phenolation leads to activation of the lignin and hence increased reaction rate during synthesis and, thus, less residual curing capacity. This relationship is well reflected by the ΔH_{tot} -data. In principle, phenolysis of large lignin molecules during phenolation modification should generally produce smaller fragments from the lignins. This in turn should result in a higher number of aromatic ring sites that are reactive towards formaldehyde and methylolated phenol monomers and oligomers. These reactive sites would be expected to readily undergo addition and condensation reactions during the subsequent resin cooking. Therefore, lignin-substituted resins that had experienced a phenolation treatment step should generally contain a smaller proportion of lower-molecular weight reactive lignin-derived fragments after synthesis and this should be reflected by a lower total residual curing capacity ΔH_{tot} . This is exactly what is observed when the ΔH_{tot} -values of the corresponding phenolated and un-phenolated lignin-phenol hybrid resin species are compared: $\Delta H_{tot,L50PF} > \Delta H_{tot,LP50PF}$, $\Delta H_{tot,K50PF} > \Delta H_{tot,KP50PF}$, and $\Delta H_{tot,K30PF} > \Delta H_{tot,KP30PF}$.

The ANOVAs given in Tabs. 8 and 9 had shown that the first exothermic peak integral, ΔH_1 is only influenced by the lignin type whereas the second exothermic peak integral, ΔH_2 only depends on the two

other factors studied, the phenolation pretreatment and the lignin substitution degree. As a result, the term ΔH_{tot} should depend on these three factors. This is, in principle, the case (Tab. 10, ANOVA for the response ΔH_{tot}). Interestingly however, when the sum $\Delta H_1 + \Delta H_2 = \Delta H_{tot}$ was analyzed, not only the effects of all single factors were statistically significant but also two of their possible synergistic interactions were found to be weakly statistically significant at a significance level of 0.05 (Tab. 10). However, although ΔH_{tot} is best described including the second-order interaction effects AB and BC, it is evident from Fig. 15 and the comparatively small values for their coefficient estimates (Tab. 10) that the interaction effects are rather weak and should not be overemphasized.

Table 10: ANOVA of the effects influencing the response ΔH_{tot} for the lignin-phenol hybrid resins

	Sum of Squares	<i>F</i> -value	<i>p</i> -value	R^2	R^2_{adjusted}	$R^2_{\text{predicted}}$
Model	10785.41	206.55	0.0048	0.9981	0.9932	0.9691
Effects				Coefficient estimates (coded):		
A: Lignin type	2108.93	201.94	0.0049			-16.24
B: Phenolation	3291.44	315.17	0.0032			+20.28
C: Substitution	4868.38	466.17	0.0021			-24.67
AB	247.20	23.67	0.0397			-5.56
BC	269.47	25.80	0.0366			+5.80
Residual	20.89					

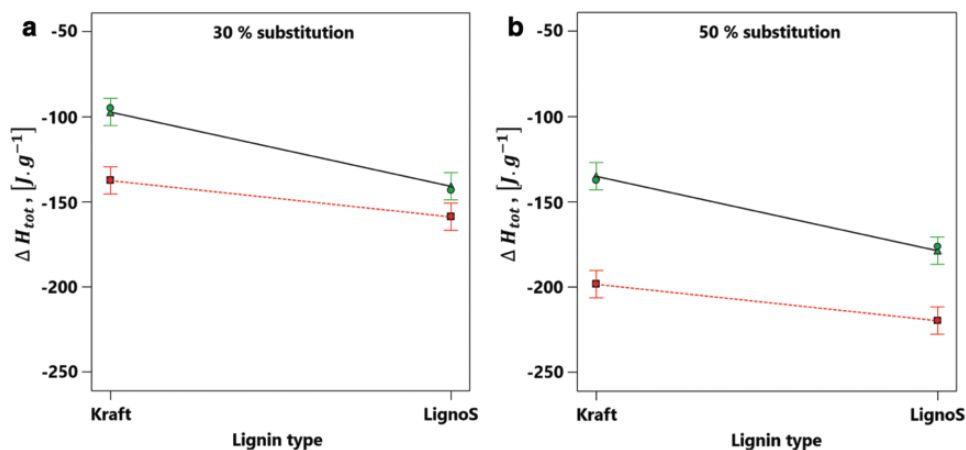


Figure 15: Two-factor interaction plot for the total residual curing capacity ΔH_{tot} of the synthesized lignin-phenol hybrid resins. (a) low level of substitution (30% lignin), (b) high level of substitution (50% lignin). The full line represents the interaction graph for the resins with phenolation treatment, the dotted red line represents the interaction graph for the resins without phenolation treatment

The residual curing capacity depends mainly on all three single factors varied in this study, the most important one being the degree of substitution of phenol by lignin. Higher levels of lignin result in larger values for total residual curing capacity. This effect is more pronounced with lignosulfonate than with Kraft lignin. If no phenolation modification is performed, resins with larger total exothermic enthalpy integrals are obtained.

4 Conclusion

Several phenolic resol resins were synthesized where phenol was substituted by different amounts of two types of lignin materials. The effect of phenolation pretreatment on the properties of these hybrid resins was studied in detail. The resulting hybrid PF resins were investigated using Fourier transform infrared spectroscopy, gel permeation chromatography, contact angle measurements, tensiometry and differential scanning calorimetry. The FTIR spectra showed the typical absorbance bands of phenolic resins and allowed to accurately determine each lignin component. The viscosities of the studied resins showed a rather complex behavior and depended strongly on the level of phenol substitution and whether a phenolation pretreatment was performed or not. With phenolation modification, the resins became generally much less viscous upon dilution with methanol although their average molecular weight was systematically higher. Phenolation treatment lead generally to an increase in the polar component of the surface energy. However, the overall contribution of the polar component to the total surface energy was comparatively low and was in the case of lignosulfonate substitution compensated by relatively larger changes in the dispersive component of the surface energy. However, the increase in surface energy was more pronounced for resins substituted by Kraft lignin than with those containing lignosulfonate. The curing behavior was modified by lignin addition, all tree investigated factors had an effect on the total residual curing capacity, ΔH_{tot} of the prepared lignin-phenol hybrid resins. While ΔH_1 was only influenced by the type of lignin, ΔH_2 was affected by the degree of substitution and phenolation treatment. The molecular weight distribution of the phenolated lignins generally showed a reduction in average molecular weight and an increase in reactivity towards condensation with phenolic resin. It was shown that the type of lignin, its content in the resin and the degree of its additional activation (phenolation), significantly influence the relative proportions of different molecular weight fractions present in the resulting oligomeric hybrid resin. Increasing the concentration of activated Kraft lignin and lignosulfonate up to 50% significantly increased the content of high-molecular weight fractions in the hybrid resins. However, the quality of the Indulin hybrid resins prepared under the same synthesis conditions was found to be not optimal in terms of polydispersity. The differences in the molar mass distribution profiles of phenolic resins, containing lignosulfonates or kraft lignin, were considered based on local variations of the pKa, and consequently the pH-microenvironment at the lignin surface segments, which are significantly dependent on the amount and the degree of dissociation of phenolic groups Ph-OH as well as chemical changes of depolymerized lignin structures. The impregnation performance of the resins studied in the present work will be subject of a subsequent study also submitted to this Journal [47].

Acknowledgement: This work was carried out within the COMET program Fun 3.3., funded by the Austrian FFG, project number 844608. The authors thank Dr. Petra Wollboldt for having participated in the phenolic resin measurements (Size Exclusion Chromatography).

Funding Statement: This work was carried out within the COMET program Fun 3.3., funded by the Austrian FFG, project number 844608.

Conflicts of Interest: The authors declare that they have no conflicts of interest to report regarding the present study.

References

1. Anonymus. (2015). *Phenolic resins for impregnation*. European Phenolic Resin Association. <http://www.epra.eu/21.html>.
2. Grenier-Loustalot, M. F., Larroque, S., Grande, D., Grenier, P., Bedel, D. (1996). Phenolic resins: 2. Influence of catalyst type on reaction mechanisms and kinetics. *Polymer*, 37(8), 1363–1369. DOI 10.1016/0032-3861(96)81133-5.

3. Thébault, M., Müller, U., Kandelbauer, A., Zikulnig-Rusch, E., Lammer, H. (2017). Review on impregnation issues in laminates manufacture: opportunities and risks of phenol substitution by lignins or other natural phenols in resins. *European Journal of Wood and Wood Products*, 75(6), 853–876. DOI 10.1007/s00107-017-1206-7.
4. Yang, W., Rallini, M., Natali, M., Kenny, J., Ma, P. et al. (2019). Preparation and properties of adhesives based on phenolic resin containing lignin micro and nanoparticles: a comparative study. *Materials and Design*, 161, 55–63. DOI 10.1016/j.matdes.2018.11.032.
5. Pilato, L. A. (2010). *Phenolic resins: a century of progress*. Berlin, Heidelberg: Springer.
6. Lundquist, K., Parkås, J. (2011). Different types of phenolic units in lignins. *BioResources*, 6, 920–926.
7. Ralph, J., Lundquist, K., Brunow, G., Lu, F., Kim, H. et al. (2004). Lignins: natural polymers from oxidative coupling of 4-hydroxyphenyl-propanoids. *Phytochemistry Reviews*, 3(1–2), 29–60. DOI 10.1023/B:PHYT.0000047809.65444.a4.
8. Ralph, J., Brunow, G., Boerjan, W. (2007). *Lignins. Encyclopedia of life sciences*. New York: John Wiley & Sons, 1–10.
9. Lapiere, C., Pollet, B., Rolando, C. (1995). New insights into the molecular architecture of hardwood lignins by chemical degradative methods. *Research on Chemical Intermediates*, 21(3–5), 397–412. DOI 10.1007/BF03052266.
10. Xu, C., Arancon, R. A. D., Labidi, J., Luque, R. (2014). Lignin depolymerisation strategies: towards valuable chemicals and fuels. *Chemical Society Reviews*, 43(22), 7485–7500. DOI 10.1039/C4CS00235K.
11. Hu, L., Pan, H., Zhou, Y., Zhang, M. (2011). Methods to improve lignin's reactivity as a phenol substitute and as replacement for other phenolic compounds: a brief review. *BioResources*, 6, 3515–3525.
12. Pietarinen, S., Ringena, O., Eskelinen, K., Valkonen, S. (2013). A method for increasing the reactivity of lignin. *WO2015044528 (A1)*.
13. Laurichesse, S., Avérous, L. (2014). Chemical modification of lignins: towards biobased polymers. *Progress in Polymer Science*, 39(7), 1266–1290. DOI 10.1016/j.progpolymsci.2013.11.004.
14. Vázquez, G., González, J., Freire, S., Antorrena, G. (1997). Effect of chemical modification of lignin on the gluebond performance of lignin-phenolic resins. *Bioresource Technology*, 60(3), 191–198. DOI 10.1016/S0960-8524(97)00030-8.
15. Ghorbani, M., Liebner, F., Van Herwijnen, H. W. G., Pfungen, L., Krahofer, M. et al. (2016). Lignin phenol formaldehyde resoles: the impact of lignin type on adhesive properties. *BioResources*, 11(3), 6727–6741. DOI 10.15376/biores.11.3.6727-6741.
16. Zhang, W., Ma, Y., Wang, C., Li, S., Zhang, M. et al. (2013). Preparation and properties of lignin-phenol-formaldehyde resins based on different biorefinery residues of agricultural biomass. *Industrial Crops and Products*, 43, 326–333. DOI 10.1016/j.indcrop.2012.07.037.
17. Mahendran, A. R., Wuzella, G., Aust, N., Müller, U., Kandelbauer, A. (2013). Processing and characterization of natural fibre reinforced composites using lignin phenolic binder. *Polymers and Polymer Composites*, 21(4), 199–206. DOI 10.1177/096739111302100401.
18. Ysbrandy, R. E., Sanderson, R. D., Gerischer, G. F. R. (1991). DSC thermal analysis of phenol and phenol-lignin extended resols and their physical behavior in paper laminates. *Papier*, 45, 62–67.
19. Ysbrandy, R. E., Sanderson, R. D., Gerischer, G. F. R. (1992). Adhesives from autohydrolysis Bagasse lignin, a renewable resource. Part I. The physical properties of laminates made with phenolated lignin Novolacs. *Holzforschung*, 46(3), 253–256. DOI 10.1515/hfsg.1992.46.3.253.
20. Mahendran, A. R., Wuzella, G., Kandelbauer, A. (2010). Thermal characterization of Kraft Lignin phenol-formaldehyde resin for paper impregnation. *Journal of Adhesion Science and Technology*, 24(8–10), 1553–1565. DOI 10.1163/016942410X500936.
21. Ghorbani, M., Mahendran, A. R., van Herwijnen, H. W. G., Liebner, F., Konnerth, J. (2017). Paper-based laminates produced with kraft lignin-rich phenol-formaldehyde resoles meet requirements for outdoor usage. *European Journal of Wood and Wood Products*, 76, 1–7.

22. Hubert, P., Poursartip, A. (1998). A review of flow and compaction modelling relevant to thermoset matrix laminate processing. *Journal of Reinforced Plastics and Composites*, 17(4), 286–318. DOI 10.1177/073168449801700402.
23. Thébault, M., Kandelbauer, A., Zikulnig-Rusch, E., Putz, R., Jury, S. et al. (2018). Impact of phenolic resin preparation on its properties and its penetration behavior in Kraft paper. *European Polymer Journal*, 104, 90–98. DOI 10.1016/j.eurpolymj.2018.05.003.
24. Thébault, M., Kandelbauer, A., Müller, U., Zikulnig-Rusch, E., Lammer, H. (2017). Factors influencing the processing and technological properties of laminates based on phenolic resin impregnated papers. *European Journal of Wood and Wood Products*, 75(5), 785–806. DOI 10.1007/s00107-017-1205-8.
25. Matsushita, Y., Wada, S., Fukushima, K., Yasuda, S. (2006). Surface characteristics of phenol–formaldehyde–lignin resin determined by contact angle measurement and inverse gas chromatography. *Industrial Crops and Products*, 23(2006), 115–121. DOI 10.1016/j.indcrop.2005.04.004.
26. Yuan, Y., Lee, T. R. (2013). Contact angle and wetting properties. *Springer Series in Surface Sciences*, 51, 3–34.
27. Anonymous. (2018). ACCU dyne test, surface tension components and molecular weight of selected liquids. https://www.accudynetest.com/surface_tension_table.html#007.
28. Figueiredo, A. B., Evtuguin, D. V., Monteiro, J., Cardoso, E. F., Mena, P. C., et al. (2011). Structure–surface property relationships of Kraft papers: implication on impregnation with phenol-formaldehyde resin. *Industrial & Engineering Chemistry Research*, 50(5), 2883–2890. DOI 10.1021/ie101912h.
29. Owens, D. K., Wendt, R. C. (1969). Estimation of the surface free energy of polymers. *Journal of Applied Polymer Science*, 13(8), 1741–1747. DOI 10.1002/app.1969.070130815.
30. Gabilondo, N., Larrañaga, M., Peña, C., Corcuera, M. A., Echeverría, J. M. et al. (2006). Polymerization of resole resins with several formaldehyde/phenol molar ratios: amine catalysts against sodium hydroxide catalysts. *Journal of Applied Polymer Science*, 102(3), 2623–2631. DOI 10.1002/app.24017.
31. Tejado, A., Peña, C., Labidi, J., Echeverría, J. M., Mondragon, I. (2007). Physico-chemical characterization of lignins from different sources for use in phenol-formaldehyde resin synthesis. *Bioresource Technology*, 98(8), 1655–1663. DOI 10.1016/j.biortech.2006.05.042.
32. Colthup, N. B. (1950). Spectra-structure correlations in the infra-red region. *Journal of the Optical Society of America*, 40(6), 397–400. DOI 10.1364/JOSA.40.000397.
33. Hergert, H. L. (1960). Infrared spectra of lignin and related compounds.II. Conifer lignin and model compounds. *Journal of Organic Chemistry*, 25(3), 405–413.
34. Norgren, M., Lindström, B. (2000). Dissociation of phenolic groups in Kraft lignin at elevated temperatures. *Holzforschung*, 54(5), 519–527. DOI 10.1515/HF.2000.088.
35. Norgren, M., Edlund, H., Wagberg, L., Lindström, B., Annergren, G. (2001). Aggregation of Kraft lignin derivatives under conditions relevant to the process. Part I. Phase behavior. *Colloids and Surfaces A: Physicochemical and Engineering Aspects*, 194, 85–96.
36. Evstigneev, E. I. (2010). Specific features of lignin dissolution in aqueous and aqueous-organic media. *Russian Journal of Applied Chemistry*, 83(3), 509–513. DOI 10.1134/S1070427210030250.
37. Sun, Y., Cheng, J. (2002). Hydrolysis of lignocellulosic materials for ethanol production: a review. *Bioresource Technology*, 83(1), 1–11. DOI 10.1016/S0960-8524(01)00212-7.
38. Guizani, C., Lachenal, D. (2017). Controlling the molecular weight of lignosulfonates by an alkaline oxidative treatment at moderate temperatures and atmospheric pressure: a size-exclusion and reverse phase chromatography study. *International Journal of Molecular Sciences*, 18(12), 2520–2538. DOI 10.3390/ijms18122520.
39. Podschun, J., Stücker, A., Saake, B., Lehnen, R. (2015). Structure-function relationships in the phenolation of lignins from different sources. *ACS Sustainable Chemistry and Engineering*, 3(10), 2526–2532. DOI 10.1021/acssuschemeng.5b00705.
40. Jiang, X., Liu, J., Du, X., Hu, Z., Chang, H. M. et al. (2018). Phenolation to improve lignin reactivity toward thermosets application. *ACS Sustainable Chemistry & Engineering*, 6(4), 5504–5512. DOI 10.1021/acssuschemeng.8b00369.

41. Ragnar, M., Lindgren, C. T., Nilvebrant, N. O. (2000). pK_a-values of guaiacyl and syringyl phenols related to lignin. *Journal of Wood Chemistry and Technology*, 20(3), 277–305. DOI 10.1080/02773810009349637.
42. Thébault, M., Kandelbauer, A., Eicher, I., Geyer, B., Zikulnig-Rusch, E. (2018). Properties data of phenolic resins synthesized for the impregnation of saturating Kraft paper. *Data in Brief*, 20, 345–352. DOI 10.1016/j.dib.2018.07.006.
43. Schindlbauer, H., Henkel, G., Weiss, J., Eichberger, W. (1975). Quantitative studies on the curing behavior of phenoplasts by means of differential thermal analysis (DSC). *Angewandte Makromolekulare Chemie*, 49(1), 115–128. DOI 10.1002/apmc.1976.050490110.
44. Chan, F., He, G., Bedard, Y., Riedl, B. (2004). Curing kinetics of phenol-formaldehyde resins. *METTLER TOLEDO Thermo Analytica User Company*, 19, 10–12.
45. Christiansen, A. W., Gollob, L. (1985). Differential scanning calorimetry of phenol-formaldehyde resins. *Journal of Applied Polymer Science*, 30(6), 2279–2289. DOI 10.1002/app.1985.070300601.
46. Park, B. D., Riedl, B., Bae, H. J., Kim, Y. S. (1999). Differential scanning calorimetry of phenol-formaldehyde (PF) adhesives. *Journal of Wood Chemistry and Technology*, 19(3), 265–286. DOI 10.1080/02773819909349612.
47. Thébault, M., Li, Y., Beuc, C., Frömel-Frybort, S., Zikulnig-Rusch, E. M. et al. (2020). Impregnated paper-based decorative laminates prepared from lignin-substituted phenolic resins. *Journal of Renewable Materials*, under review.